

# Lepton-specific inert two-Higgs-doublet model confronted with the new results for muon and electron $g-2$ anomalies and multi-lepton searches at the LHC

Xiao-Fang Han<sup>1</sup>, Tianjun Li<sup>2,3</sup>, Hong-Xin Wang<sup>1</sup>, Lei Wang<sup>1</sup>, Yang Zhang<sup>4</sup>

<sup>1</sup> *Department of Physics, Yantai University, Yantai 264005, P. R. China*

<sup>2</sup> *CAS Key Laboratory of Theoretical Physics, Institute of Theoretical Physics, Chinese Academy of Sciences, Beijing 100190, P. R. China*

<sup>3</sup> *School of Physical Sciences, University of Chinese Academy of Sciences, Beijing 100049, P. R. China*

<sup>4</sup> *School of Physics and Microelectronics, Zhengzhou University, Zhengzhou 450001, P. R. China*

(Dated: April 16, 2021)

## Abstract

Combining the multi-lepton searches at the LHC, we study the possibilities of accommodating the new data of muon and electron  $g - 2$  anomalies in the lepton-specific inert two-Higgs-doublet model. We take the heavy CP-even Higgs as the 125 GeV Higgs, and find the muon and electron  $g - 2$  anomalies can be explained simultaneously in the region of  $5 \text{ GeV} < m_h < 60 \text{ GeV}$ ,  $200 \text{ GeV} < m_A < 620 \text{ GeV}$ ,  $190 \text{ GeV} < m_{H^\pm} < 620 \text{ GeV}$  for appropriate Yukawa couplings between leptons and inert Higgs. Meanwhile, the model can give a better fit to the data of lepton universality in  $\tau$  decays than the SM. Further, the multi-lepton event searches at the LHC impose a stringent upper bound on  $m_h$ ,  $m_h < 35 \text{ GeV}$ .

## I. INTRODUCTION

The Fermilab collobartion presented their new result for muon anomalous magnetic moment which now, combined with the data of the E821 [1, 2], amounts to [3]

$$\Delta a_\mu = a_\mu^{exp} - a_\mu^{SM} = (251 \pm 59) \times 10^{-11}. \quad (1)$$

The experimental value has an approximate  $4.2\sigma$  discrepancy from the SM prediction [4–7]. Besides, an improvement in the measured mass of atomic Cesium used in conjunction with other known mass ratios and the Rydberg constant leads to the most precise value of the fine structure constant [8]. As a result, the experimental value of the electron  $g - 2$  has a  $2.4\sigma$  deviation from the SM prediction [9, 10],

$$\Delta a_e = a_e^{exp} - a_e^{SM} = (-87 \pm 36) \times 10^{-14}, \quad (2)$$

which is opposite in sign from the muon  $g - 2$ .

The lepton-specific two-Higgs-doublet model (2HDM) can explain muon  $g - 2$  anomaly simply [11–26], but will raise the discrepancy in lepton flavor universality (LFU) in  $\tau$  decay [21–23]. In addition, the muon and electron  $g - 2$  anomalies can not be explained simultaneously in lepton-specific 2HDM since there is an opposite sign between them. There have been some new physics models which attempt to explain the muon and electron  $g - 2$  simultaneously [27–54]. In Ref. [31], we propose a lepton-specific inert 2HDM to explain the muon and electron  $g - 2$  anomalies, and the key point is that these Yukawa couplings for  $\mu$  and  $e/\tau$  have opposite sign. In the model, the extra Higgses will decay into leptons mainly. Therefore, the multi-lepton event searches at the LHC can impose stringent constraints on the model. Motivated by the new results for muon  $g - 2$  and multi-lepton event searches at the LHC, we revisit the possibilities of accommodating muon and electron  $g - 2$  anomalies in the lepton-specific inert 2HDM. In this paper, we study a different scenario from that of Ref. [31], and take the inert CP-even Higgs  $h$  to be lighter than the SM-like Higgs  $H$ . In such scenario, a very light CP-even Higgs  $h$  plays important roles in explaining the muon and electron  $g-2$  anomalies, and is expected to more easily avoid the constraints from the multi-lepton searches at the LHC than the scenario of Ref. [31] in which  $h$  is heavier than the 125 GeV Higgs.

Our work is organized as follows. In Sec. II we will give a brief introduction on the model.

In Sec. III and Sec. IV, we introduce the numerical calculations, and show the allowed and excluded parameter space. Finally, we give our conclusion in Sec. V.

## II. LEPTON-SPECIFIC INERT 2HDM

We add an inert Higgs doublet field to the SM, and the scalar potential is written as,

$$\begin{aligned}
V = & Y_1(\Phi_1^\dagger\Phi_1) + Y_2(\Phi_2^\dagger\Phi_2) + \frac{\lambda_1}{2}(\Phi_1^\dagger\Phi_1)^2 + \frac{\lambda_2}{2}(\Phi_2^\dagger\Phi_2)^2 \\
& + \lambda_3(\Phi_1^\dagger\Phi_1)(\Phi_2^\dagger\Phi_2) + \lambda_4(\Phi_1^\dagger\Phi_2)(\Phi_2^\dagger\Phi_1) \\
& + \left[ \frac{\lambda_5}{2}(\Phi_1^\dagger\Phi_2)^2 + \text{h.c.} \right].
\end{aligned} \tag{3}$$

Here we impose a discrete  $Z_2$  symmetry under which  $\Phi_2$  is odd and the SM fields are even. We study the CP-conserving case where all  $\lambda_i$  are real. The two complex scalar doublets with the hypercharge  $Y = 1$  can be given as

$$\Phi_1 = \begin{pmatrix} G^+ \\ \frac{1}{\sqrt{2}}(v + H + iG_0) \end{pmatrix}, \quad \Phi_2 = \begin{pmatrix} H^+ \\ \frac{1}{\sqrt{2}}(h + iA) \end{pmatrix}. \tag{4}$$

The  $\Phi_1$  field has the vacuum expectation value (VEV)  $v = 246$  GeV, and the VEV of  $\Phi_2$  field is zero. The  $Y_1$  is determined by the scalar potential minimum condition,

$$Y_1 = -\frac{1}{2}\lambda_1 v^2. \tag{5}$$

The Nambu-Goldstone bosons  $G^0$  and  $G^+$  are eaten by the gauge bosons. The  $H^+$  and  $A$  are the mass eigenstates of the charged Higgs boson and CP-odd Higgs boson. Their masses are given as

$$m_{H^\pm}^2 = Y_2 + \frac{\lambda_3}{2}v^2, \quad m_A^2 = m_{H^\pm}^2 + \frac{1}{2}(\lambda_4 - \lambda_5)v^2. \tag{6}$$

The  $H$  is the SM-like Higgs, and has no mixing with the inert CP-even Higgs  $h$ . Their masses are given as

$$m_H^2 = \lambda_1 v^2 \equiv (125 \text{ GeV})^2, \quad m_h^2 = m_A^2 + \lambda_5 v^2. \tag{7}$$

The fermions obtain the mass terms from the Yukawa interactions with  $\Phi_1$ ,

$$-\mathcal{L} = y_u \bar{Q}_L \tilde{\Phi}_1 u_R + y_d \bar{Q}_L \Phi_1 d_R + y_l \bar{L}_L \Phi_1 e_R + \text{h.c.}, \tag{8}$$

where  $Q_L^T = (u_L, d_L)$ ,  $L_L^T = (\nu_L, l_L)$ ,  $\tilde{\Phi}_1 = i\tau_2\Phi_1^*$ , and  $y_u$ ,  $y_d$  and  $y_\ell$  are  $3 \times 3$  matrices in family space. In addition, in the lepton sector we introduce the  $Z_2$  symmetry-breaking Yukawa interactions of  $\Phi_2$ ,

$$\begin{aligned}
-\mathcal{L} = & \frac{\sqrt{2}m_e}{v} \kappa_e \bar{L}_{1L} \Phi_2 e_R + \frac{\sqrt{2}m_\mu}{v} \kappa_\mu \bar{L}_{2L} \Phi_2 \mu_R \\
& + \frac{\sqrt{2}m_\tau}{v} \kappa_\tau \bar{L}_{3L} \Phi_2 \tau_R + \text{h.c.} .
\end{aligned} \tag{9}$$

We can obtain the lepton Yukawa couplings of extra Higgses ( $h$ ,  $A$ , and  $H^\pm$ ) from Eq. (9). The neutral Higgses  $h$  and  $A$  have no couplings to  $ZZ$ ,  $WW$ . At the tree-level, the SM-like Higgs  $H$  has the same couplings to fermions and gauge bosons as the SM.

### III. NUMERICAL CALCULATIONS

In the lepton-specific 2HDM and aligned 2HDM,  $\kappa_\tau$  equals to  $\kappa_\mu$ . As a result, the decay  $\tau \rightarrow \mu\nu\nu$  will obtain negative contribution from the diagram mediated by the charged Higgs. In the model we take  $\kappa_\mu$  to be opposite in sign from  $\kappa_\tau$ . Thus, the diagrams mediated by the charged Higgs produce positive contribution to the decay  $\tau \rightarrow \mu\nu\nu$ , and the model can give better fit to the data of the LUF in the  $\tau$  decay. When  $\kappa_\mu$  is opposite in sign from  $\kappa_\tau$ , the contributions of the CP-even (CP-odd) Higgses to muon  $g - 2$  are positive (negative) at the two-loop level and positive (negative) at one-loop level. Therefore, we take the heavy CP-even Higgs as the 125 GeV Higgs,  $m_H = 125$  GeV, and make the light CP-even Higgs  $h$  to be light enough to enhance muon  $g - 2$ . Since electron  $g - 2$  is opposite in sign from muon  $g - 2$ , we will take  $\kappa_e$  to have a opposite sign from  $\kappa_\mu$ .

In our calculations, we take  $\lambda_2$ ,  $\lambda_3$ ,  $m_H$ ,  $m_h$ ,  $m_A$  and  $m_{H^\pm}$  as the input parameters. According to Eqs. (6, 7), the values of  $\lambda_1$ ,  $\lambda_5$  and  $\lambda_4$  can be determined.  $\lambda_2$  controls the quartic couplings of extra Higgses, and does not affect the observables considered in our paper. We take  $\lambda_3 = \lambda_4 + \lambda_5$  to make the  $Hhh$  coupling to be absent.

We scan over several key parameters in the following ranges:

$$\begin{aligned}
5\text{GeV} < m_h < 60 \text{ GeV}, \quad 200\text{GeV} < m_A < 800\text{GeV}, \quad 90\text{GeV} < m_{H^\pm} < 800\text{GeV}, \\
1 < \kappa_\tau < 140, \quad -200 < \kappa_\mu < -1, \quad 1 < \kappa_e < 500.
\end{aligned} \tag{10}$$

In such ranges of  $\kappa_\tau$ ,  $\kappa_\mu$  and  $\kappa_e$ , the corresponding Yukawa couplings do not become non-perturbative.

The model gives the new contributions to muon  $g - 2$  via the one-loop diagrams and the two-loop Barr-Zee diagrams involving extra Higgses. For the one-loop contributions [11] we have

$$\Delta a_\mu^{2\text{HDM}}(\text{1loop}) = \frac{m_\mu^2}{8\pi^2 v^2} \sum_i \kappa_\mu^2 r_\mu^i F_j(r_\mu^i), \quad (11)$$

where  $i = h, A, H^\pm$ ,  $r_\mu^i = m_\mu^2/M_j^2$ . For  $r_\mu^i \ll 1$  we have

$$F_h(r) \simeq -\ln r - 7/6, \quad F_A(r) \simeq \ln r + 11/6, \quad F_{H^\pm}(r) \simeq -1/6. \quad (12)$$

The contributions of the two-loop diagrams with a closed fermion loop are given by

$$\Delta a_\mu^{2\text{HDM}}(\text{2loop}) = \frac{m_\mu^2}{8\pi^2 v^2} \frac{\alpha_{\text{em}}}{\pi} \sum_{i,\ell} Q_\ell^2 \kappa_\mu \kappa_\ell r_\ell^i G_i(r_\ell^i), \quad (13)$$

where  $i = h, A, \ell = \tau$ , and  $m_\ell$  and  $Q_\ell$  are the mass and electric charge of the lepton  $\ell$  in the loop. The functions  $G_i(r)$  are [12, 13]

$$G_h(r) = \int_0^1 dx \frac{2x(1-x) - 1}{x(1-x) - r} \ln \frac{x(1-x)}{r}, \quad (14)$$

$$G_A(r) = \int_0^1 dx \frac{1}{x(1-x) - r} \ln \frac{x(1-x)}{r}. \quad (15)$$

In our calculation, we also include the contributions of the two-loop diagrams with a closed charged Higgs loop, and find that their contributions are much smaller than those of fermion loop. The calculation of  $\Delta a_e$  is similar to that of  $\Delta a_\mu$ , and we include the contributions of the two-loop diagrams with closed  $\mu$  loop and  $\tau$  loop.

The HFAG collaboration reported three ratios from pure leptonic processes, and two ratios from semi-hadronic processes,  $\tau \rightarrow \pi/K \nu$  and  $\pi/K \rightarrow \mu \nu$  [55]:

$$\begin{aligned} \left(\frac{g_\tau}{g_\mu}\right) &= 1.0011 \pm 0.0015, & \left(\frac{g_\tau}{g_e}\right) &= 1.0029 \pm 0.0015, \\ \left(\frac{g_\mu}{g_e}\right) &= 1.0018 \pm 0.0014, & \left(\frac{g_\tau}{g_\mu}\right)_\pi &= 0.9963 \pm 0.0027, \\ \left(\frac{g_\tau}{g_\mu}\right)_K &= 0.9858 \pm 0.0071, \end{aligned} \quad (16)$$

with the following definitions

$$\begin{aligned} \left(\frac{g_\tau}{g_\mu}\right)^2 &\equiv \bar{\Gamma}(\tau \rightarrow e\nu\bar{\nu})/\bar{\Gamma}(\mu \rightarrow e\nu\bar{\nu}), \\ \left(\frac{g_\tau}{g_e}\right)^2 &\equiv \bar{\Gamma}(\tau \rightarrow \mu\nu\bar{\nu})/\bar{\Gamma}(\mu \rightarrow e\nu\bar{\nu}), \\ \left(\frac{g_\mu}{g_e}\right)^2 &\equiv \bar{\Gamma}(\tau \rightarrow \mu\nu\bar{\nu})/\bar{\Gamma}(\tau \rightarrow e\nu\bar{\nu}). \end{aligned} \quad (17)$$

Where  $\bar{\Gamma}$  denotes the partial width normalized to its SM value. The correlation matrix for the above five observables is

$$\begin{pmatrix} 1 & +0.53 & -0.49 & +0.24 & +0.12 \\ +0.53 & 1 & +0.48 & +0.26 & +0.10 \\ -0.49 & +0.48 & 1 & +0.02 & -0.02 \\ +0.24 & +0.26 & +0.02 & 1 & +0.05 \\ +0.12 & +0.10 & -0.02 & +0.05 & 1 \end{pmatrix}. \quad (18)$$

In the model, we have the ratios

$$\begin{aligned} \left(\frac{g_\tau}{g_\mu}\right)^2 &\approx \frac{1 + 2\delta_{\text{loop}}^\tau}{1 + 2\delta_{\text{loop}}^\mu}, \\ \left(\frac{g_\tau}{g_e}\right)^2 &\approx \frac{1 + 2\delta_{\text{tree}} + 2\delta_{\text{loop}}^\tau}{1 + 2\delta_{\text{loop}}^\mu}, \\ \left(\frac{g_\mu}{g_e}\right)^2 &\approx 1 + 2\delta_{\text{tree}}, \\ \left(\frac{g_\tau}{g_\mu}\right)_\pi^2 &= \left(\frac{g_\tau}{g_\mu}\right)_K^2 = \left(\frac{g_\tau}{g_\mu}\right)^2. \end{aligned} \quad (19)$$

The  $\delta_{\text{tree}}$  and  $\delta_{\text{loop}}^{\tau,\mu}$  are respectively corrections from the tree-level diagrams and the one-loop diagrams mediated by the charged Higgs. They are given as [21, 23, 24]

$$\delta_{\text{tree}} = \frac{m_\tau^2 m_\mu^2 \kappa_\tau^2 \kappa_\mu^2}{8m_{H^\pm}^4} - \frac{m_\mu^2}{m_{H^\pm}^2} \kappa_\tau \kappa_\mu \frac{g(m_\mu^2/m_\tau^2)}{f(m_\mu^2/m_\tau^2)}, \quad (20)$$

$$\delta_{\text{loop}}^{\tau,\mu} = \frac{1}{16\pi^2} \frac{m_{\tau,\mu}^2}{v^2} \kappa_{\tau,\mu}^2 \left[ 1 + \frac{1}{4} (H(x_A) + H(x_h)) \right], \quad (21)$$

where  $f(x) \equiv 1 - 8x + 8x^3 - x^4 - 12x^2 \ln(x)$ ,  $g(x) \equiv 1 + 9x - 9x^2 - x^3 + 6x(1+x) \ln(x)$  and  $H(x_\phi) \equiv \ln(x_\phi)(1+x_\phi)/(1-x_\phi)$  with  $x_\phi = m_\phi^2/m_{H^\pm}^2$ .

We perform  $\chi_\tau^2$  calculation for the five observables. The covariance matrix constructed from the data of Eq. (16) and Eq. (18) has a vanishing eigenvalue, and the corresponding degree is removed in our calculation. In our discussions we require the value of  $\chi_\tau^2$  to be smaller than the SM value,  $\chi_\tau^2(\text{SM}) = 12.3$ .

The measured values of the ratios of the leptonic  $Z$  decay branching fractions are given as [56]:

$$\begin{aligned} \frac{\Gamma_{Z \rightarrow \mu^+ \mu^-}}{\Gamma_{Z \rightarrow e^+ e^-}} &= 1.0009 \pm 0.0028, \\ \frac{\Gamma_{Z \rightarrow \tau^+ \tau^-}}{\Gamma_{Z \rightarrow e^+ e^-}} &= 1.0019 \pm 0.0032, \end{aligned} \quad (22)$$

with a correlation of +0.63. In the model, the width of  $Z \rightarrow \tau^+ \tau^-$  can have sizable deviation from the SM value due to the loop contributions of the extra Higgs bosons, because they strongly interact with charged leptons. The quantities of Eq. (22) are calculated in the model are similar to Refs. [21, 23, 24].

$$\begin{aligned}\frac{\Gamma_{Z \rightarrow \mu^+ \mu^-}}{\Gamma_{Z \rightarrow e^+ e^-}} &\approx 1.0 + \frac{2g_L^e \text{Re}(\delta g_L^{2\text{HDM}}) + 2g_R^e \text{Re}(\delta g_R^{2\text{HDM}})}{g_L^e{}^2 + g_R^e{}^2} \frac{m_\mu^2 \kappa_\mu^2}{m_\tau^2 \kappa_\tau^2}, \\ \frac{\Gamma_{Z \rightarrow \tau^+ \tau^-}}{\Gamma_{Z \rightarrow e^+ e^-}} &\approx 1.0 + \frac{2g_L^e \text{Re}(\delta g_L^{2\text{HDM}}) + 2g_R^e \text{Re}(\delta g_R^{2\text{HDM}})}{g_L^e{}^2 + g_R^e{}^2}.\end{aligned}\quad (23)$$

where the SM value  $g_L^e = -0.27$  and  $g_R^e = 0.23$ .  $\delta g_L^{2\text{HDM}}$  and  $\delta g_R^{2\text{HDM}}$  are given as

$$\begin{aligned}\delta g_L^{2\text{HDM}} &= \frac{1}{16\pi^2} \frac{m_\tau^2}{v^2} \kappa_\tau^2 \left\{ -\frac{1}{2} B_Z(r_A) - \frac{1}{2} B_Z(r_h) - 2C_Z(r_A, r_h) \right. \\ &\quad \left. + s_W^2 \left[ B_Z(r_A) + B_Z(r_h) + \tilde{C}_Z(r_A) + \tilde{C}_Z(r_h) \right] \right\}, \\ \delta g_R^{2\text{HDM}} &= \frac{1}{16\pi^2} \frac{m_\tau^2}{v^2} \kappa_\tau^2 \left\{ 2C_Z(r_A, r_h) - 2C_Z(r_{H^\pm}, r_{H^\pm}) + \tilde{C}_Z(r_{H^\pm}) \right. \\ &\quad - \frac{1}{2} \tilde{C}_Z(r_A) - \frac{1}{2} \tilde{C}_Z(r_h) + s_W^2 \left[ B_Z(r_A) + B_Z(r_h) + 2B_Z(r_{H^\pm}) \right. \\ &\quad \left. \left. + \tilde{C}_Z(r_A) + \tilde{C}_Z(r_h) + 4C_Z(r_{H^\pm}, r_{H^\pm}) \right] \right\},\end{aligned}\quad (24)$$

where  $r_\phi = m_\phi^2/m_Z^2$  with  $\phi = A, h, H^\pm$ , and

$$B_Z(r) = -\frac{\Delta_\epsilon}{2} - \frac{1}{4} + \frac{1}{2} \log(r), \quad (25)$$

$$C_Z(r_1, r_2) = \frac{\Delta_\epsilon}{4} - \frac{1}{2} \int_0^1 dx \int_0^x dy \log[r_2(1-x) + (r_1-1)y + xy], \quad (26)$$

$$\begin{aligned}\tilde{C}_Z(r) &= \frac{\Delta_\epsilon}{2} + \frac{1}{2} - r[1 + \log(r)] + r^2[\log(r) \log(1+r^{-1}) \\ &\quad - \text{Li}_2(-r^{-1})] - \frac{i\pi}{2} [1 - 2r + 2r^2 \log(1+r^{-1})].\end{aligned}\quad (27)$$

The 125 GeV Higgs ( $H$ ) has the same tree-level couplings to the fermions and gauge bosons as the SM, and the  $H \rightarrow hh$  decay is absent for  $\lambda_3 = \lambda_4 + \lambda_5$ . Since the extra Higgses have no coupling to quarks, we can safely neglect the constraints from the meson observable. We employ the 2HDMC [57] to implement theoretical constraints from the vacuum stability, unitarity and coupling-constant perturbativity, as well as the constraints from the oblique parameters ( $S, T, U$ ). Adopting the recent fit results in Ref. [58], we use the following values of  $S, T, U$ ,

$$S = 0.02 \pm 0.10, \quad T = 0.07 \pm 0.12, \quad U = 0.00 \pm 0.09. \quad (28)$$

The correlation coefficients are given by

$$\rho_{ST} = 0.92, \quad \rho_{SU} = -0.66, \quad \rho_{TV} = -0.86. \quad (29)$$

HiggsBounds [59] is employed to implement the exclusion constraints from the searches for the neutral and charged Higgs at the LEP at 95% confidence level.

The extra Higgs bosons are dominantly produced at the LHC via the following electroweak processes:

$$pp \rightarrow Z^* \rightarrow hA, \quad (30)$$

$$pp \rightarrow W^{\pm*} \rightarrow H^{\pm}h, \quad (31)$$

$$pp \rightarrow W^{\pm*} \rightarrow H^{\pm}A, \quad (32)$$

$$pp \rightarrow Z^*/\gamma^* \rightarrow H^+H^-, \quad (33)$$

$$pp \rightarrow Z \rightarrow \tau^+\tau^-h. \quad (34)$$

In our scenario, the main decay modes of the Higgs bosons are

$$h \rightarrow \tau^+\tau^-, \mu^+\mu^-, \dots, \quad (35)$$

$$A \rightarrow \tau^+\tau^-, Zh, \mu^+\mu^-, \dots, \quad (36)$$

$$H^{\pm} \rightarrow \tau^{\pm}\nu, W^{\pm}h, \mu^{\pm}\nu, \dots. \quad (37)$$

We perform simulations for the processes using MG5\_aMC-2.4.3 [60] with PYTHIA6 [61] and Delphes-3.2.0 [62], and impose the constraints from all the analysis at the 13 TeV LHC in the latest CheckMATE 2.0.28 [63], as well as analysis we implemented in our previous works [31, 64]. Besides, we also impose the recently published analyses of searching for events with three or more leptons, with up to two hadronical  $\tau$  leptons, using 13 TeV LHC 137 fb<sup>-1</sup> data [65]. It improves the limits on chargino mass in a simplified SUSY model that wino-like chargino/neutralino decaying to  $\tau$ s. The signal regions of 41I, 41J and 41K give strongest constraints on our samples, which require 4 leptons with one or two hadronical  $\tau$  leptons in the final states, because of the dominated multi-lepton final states in our model.

#### IV. RESULTS AND DISCUSSIONS

After imposing the constraints of "pre-muon  $g - 2$ " (denoting the theory, the oblique parameters, the exclusion limits from the searches for Higgs at LEP), in Fig. 1 we show the



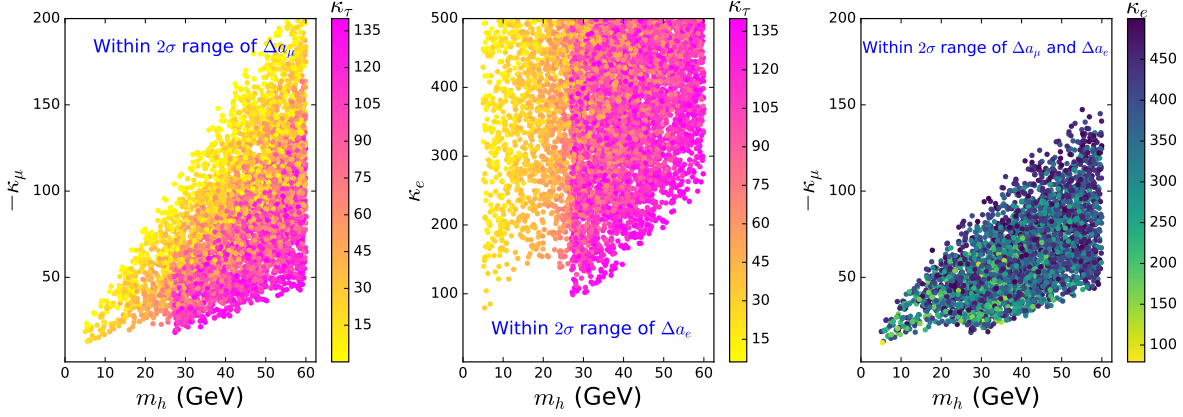


FIG. 1: The samples within  $2\sigma$  ranges of  $\Delta a_\mu$  (left panel),  $\Delta a_e$  (middle panel), and both  $\Delta a_\mu$  and  $\Delta a_e$  (right panel). All the samples satisfy the constraints of "pre-muon  $g - 2$ ".

surviving samples which are consistent with  $\Delta a_\mu$  and  $\Delta a_e$  at the  $2\sigma$  level. Both one-loop and two-loop diagrams give positive contributions to  $\Delta a_\mu$ . For  $\Delta a_e$ , the contributions of one-loop are positive and those of two-loop are negative. Only the contributions of two-loop can make  $\Delta a_e$  to be within  $2\sigma$  range for large enough  $\kappa_\tau \kappa_e$ .  $\Delta a_\mu$  and  $\Delta a_e$  respectively favor  $-\kappa_\mu$  and  $\kappa_e$  to increase with  $m_h$ . For  $\kappa_\tau = 140$  and  $m_h = 60$  GeV,  $-\kappa_\mu$  and  $\kappa_e$  are respectively required to be larger than 40 and 250. Due to the constraints from the searches for  $ee \rightarrow \tau\tau(h) \rightarrow \tau\tau\tau\tau$  at LEP [66],  $\kappa_\tau$  is required to be smaller than 90 for  $m_h < 27$  GeV. As a result, the relative large  $-\kappa_\mu$  and  $\kappa_e$  are respectively required to explain  $\Delta a_\mu$  and  $\Delta a_e$  for  $m_h < 27$  GeV. The right panel shows that the upper limits of  $-\kappa_\mu$  within the  $2\sigma$  ranges of both  $\Delta a_\mu$  and  $\Delta a_e$  are much smaller than those within the  $2\sigma$  ranges of  $\Delta a_\mu$ . This is because  $\kappa_\tau$  is required to be large enough to explain  $\Delta a_e$ , and for such large  $\kappa_\tau$ ,  $\Delta a_\mu$  favors a relative small  $\kappa_\mu$ .

After imposing the constraints of "pre-muon  $g - 2$ ", we show the surviving samples with  $\chi_\tau^2 < 12.3$  in Fig. 2. Because  $\kappa_\mu$  is opposite in sign from  $\kappa_\tau$ , the second term of  $\delta_{\text{tree}}$  in Eq. (20) is positive, which gives a well fit to  $g_\tau/g_e$ . Such case is not realized in the lepton-specific 2HDM and aligned 2HDM. From Fig. 2, we find that  $\chi_\tau^2$  increases with  $m_{H^\pm}$ , and obtains a relative small value for the moderate  $-\kappa_\mu \kappa_\tau$ . The  $\chi_\tau^2$  can be as low as 7.4, which is much smaller than the SM value.

In Fig. 3 we show the surviving samples after imposing the constraints of "pre-muon  $g - 2$ ",  $\Delta a_\mu$ ,  $\Delta a_e$ ,  $\chi_\tau^2 < 12.3$ ,  $Z$  decays, and the direct searches at LHC. The Fig. 3 shows that the points with relatively larger  $m_A/m_{H^\pm}$  or lower  $m_h$  can escape the direct searches.

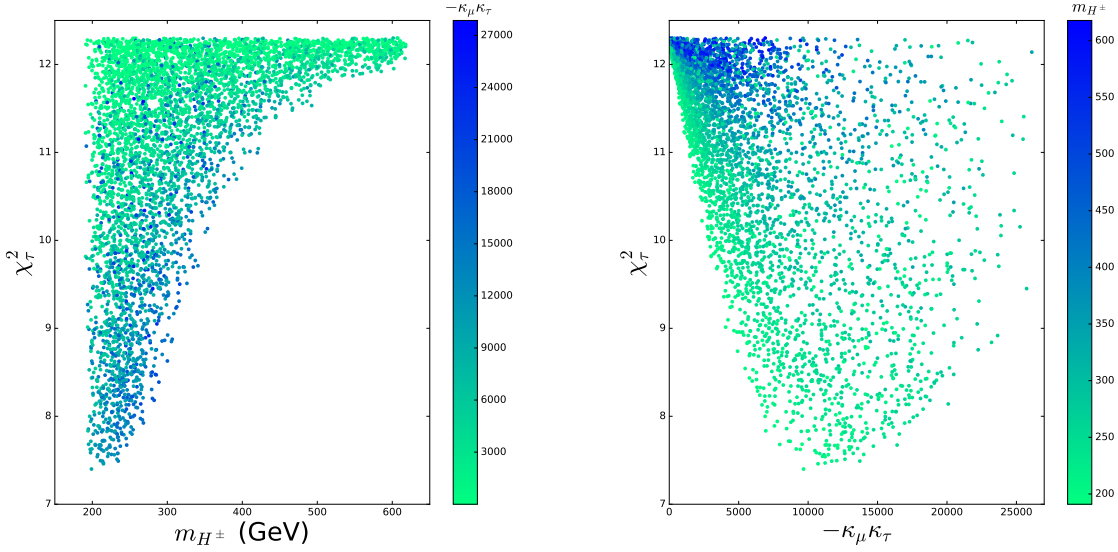


FIG. 2: The surviving samples fit the data of LFU in  $\tau$  decay with  $\chi^2_\tau < 12.3$ . All the samples satisfy the constraints of "pre-muon  $g - 2$ ".

The production cross sections at the LHC decrease with heavier  $A/H^\pm$ , and this region can be further detected with higher luminosity and collision energy. For the light  $h$ , the  $\tau$ s from  $h$  in decays become too soft to be distinguished at detector, while the  $\tau$ s from  $h$  in  $A/H^\pm$  decays are collinear because of the large mass splitting between  $h$  and  $A/H^\pm$ . Meanwhile, the  $A/H^\pm \rightarrow hZ/W^\pm$  decay modes dominate the  $A/H^\pm$  decays in the low  $m_h$  region. Thus, in the region of  $m_h < 20$  GeV, the acceptance of above signal region for final state of two collinear  $\tau + Z/W$  boson quickly decreases.

The upper-right panel of Fig. 3 shows that the  $\chi^2_\tau$  is required to be closed to the SM value since the multi-lepton event searches at the LHC favor large  $m_{H^\pm}$  or small  $m_h$ . For small  $m_h$ , the muon and electron anomalies favor small  $\kappa_\tau$  and  $-\kappa_\mu$ . As a result, the new contribution to  $\chi^2_\tau$  are sizably reduced. The  $\chi^2_\tau$  is allowed to be as low as 11.5 for  $m_{H^\pm}$  around 200 GeV, which is visibly smaller than the SM value, 12.3. The Fig. 3 shows that the parameters of the Yukawa couplings are favored in the region of  $15 < -\kappa_\mu < 90$ ,  $5 < \kappa_\tau < 50$ , and  $160 < \kappa_e < 500$ .

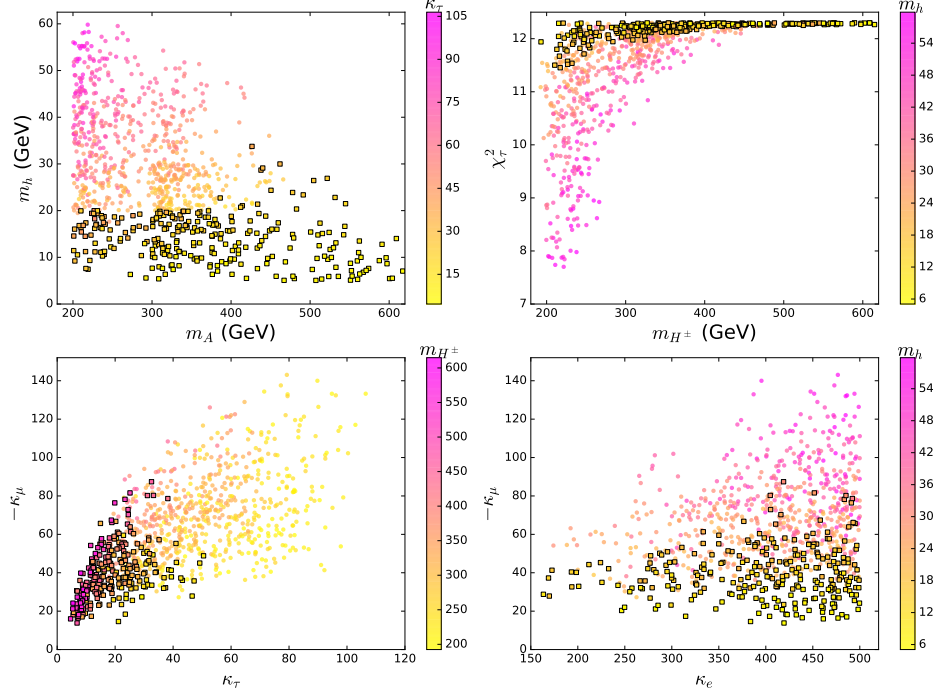


FIG. 3: The allowed samples (squares) and excluded samples (bullets) by the direct search limits from the LHC at 95% confidence level. All the samples satisfy the constraints of "pre-muon  $g-2$ ",  $\Delta a_\mu$ ,  $\Delta a_e$ ,  $\chi_\tau^2 < 12.3$ , and  $Z$  decays.

## V. CONCLUSION

In the lepton-specific inert two-Higgs-doublet model, we consider relevant theoretical and experimental constraints, especially for the multi-lepton event searches at the LHC, and discuss the possibilities of explaining the new muon  $g-2$  anomaly reported by the Fermilab and electron  $g-2$  anomaly. We find that the muon and electron  $g-2$  anomalies can be explained simultaneously in the region of  $5 \text{ GeV} < m_h < 35 \text{ GeV}$ ,  $200 \text{ GeV} < m_A < 620 \text{ GeV}$ ,  $190 \text{ GeV} < m_{H^\pm} < 620 \text{ GeV}$ ,  $15 < -\kappa_\mu < 90$ ,  $5 < \kappa_\tau < 50$ , and  $160 < \kappa_e < 500$ .

## Acknowledgment

This work was supported by the National Natural Science Foundation of China under grant 11975013 and 11875062, and by the Project of Shandong Province Higher Educational

- [1] G. W. Bennett et al. [Muon g-2 Collaboration], Phys. Rev. Lett. **86**, (2001) 2227.
- [2] G. W. Bennett et al. [Muon g-2 Collaboration], Phys. Rev. D **73**, (2006) 072003.
- [3] B. Abi *et al.* [Fermilab Collaboration], Phys. Rev. Lett. **126**, (2021) 141801.
- [4] T. Aoyama, M. Hayakawa, T. Kinoshita and M. Nio, Phys. Rev. Lett. **109**, (2012) 111808.
- [5] A. Czarnecki, W. J. Marciano and A. Vainshtein, Phys. Rev. D **67**, (2003) 073006.
- [6] G. Eichmann, C. S. Fischer and R. Williams, Phys. Rev. D **101**, (2020) 054015.
- [7] M. Davier, A. Hoecker, B. Malaescu and Z. Zhang, Eur. Phys. Jour. C **80**, (2020) 241.
- [8] R. H. Parker, C. Yu, W. Zhong, B. Estey, H. Mueller, Science **360**, (2018) 191.
- [9] D. Hanneke, S. Fogwell and G. Gabrielse, Phys. Rev. Lett. **100**, 120801 (2008).
- [10] D. Hanneke, S. F. Hoogerheide and G. Gabrielse, Phys. Rev. A **83**, 052122 (2011).
- [11] A. Dedes and H. E. Haber, JHEP **0105**, (2001) 006.
- [12] D. Chang, W.-F. Chang, C.-H. Chou, and W.-Y. Keung, Phys. Rev. D **63**, (2001) 091301.
- [13] K. M. Cheung, C. H. Chou and O. C. W. Kong, Phys. Rev. D **64**, (2001) 111301.
- [14] J. Cao, P. Wan, L. Wu and J. M. Yang, Phys. Rev. D **80**, (2009) 071701.
- [15] L. Wang and X. F. Han, JHEP **05**, (2015) 039.
- [16] E. J. Chun, Z. Kang, M. Takeuchi, Y.-L. Tsai, JHEP **1511**, (2015) 099.
- [17] T. Han, S. K. Kang, J. Sayre, JHEP **1602**, (2016) 097.
- [18] V. Ilisie, JHEP **1504**, (2015) 077.
- [19] A. Cherchiglia, P. Kneschke, D. Stockinger, H. Stockinger-Kim, JHEP **1701**, (2017) 007.
- [20] X. Liu, L. Bian, X.-Q. Li, J. Shu, Nucl. Phys. B **909**, (2016) 507-524.
- [21] T. Abe, R. Sato and K. Yagyu, JHEP **1507**, (2015) 064.
- [22] A. Crivellin, J. Heeck, P. Stoffer, Phys. Rev. Lett. **116**, (2016) 081801.
- [23] E. J. Chun, J. Kim, JHEP **1607**, (2016) 110.
- [24] L. Wang, J. M. Yang, M. Zhang, Y. Zhang, Phys. Lett. B **788**, (2019) 519-529.
- [25] D. Sabatta, A. S. Cornell, A. Goyal, M. Kumar, B. Mellado, Chin. Phys. C **44**, (2020) 063103.
- [26] E. J. Chun, T. Mondal, Phys. Lett. B **802**, (2020) 135190.
- [27] H. Davoudiasl, W. J. Marciano, Phys. Rev. D **98**, (2018) 075011.
- [28] J.-J. Zhang, M. He, X.-G. He, G. Li, Nucl. Phys. B **953**, (2020) 114968.

- [29] A. Crivellin, M. Hoferichter, P. Schmidt-Wellenburg, *Phys. Rev. D* **98**, (2018) 113002.
- [30] J. Liu, C. E. M. Wagner, X.-P. Wang, *JHEP* **1903**, (2019) 008.
- [31] X.-F. Han, T. Li, L. Wang, Y. Zhang, *Phys. Rev. D* **99**, (2019) 095034.
- [32] M. Endo, W. Yin, *JHEP* **1908**, (2019) 122.
- [33] H. Davoudiasl, W. J. Marciano, *Phys. Rev. D* **98**, (2018) 075011.
- [34] M. Abdullah, B. Dutta, S. Ghosh, T. Li, *Phys. Rev. D* **100**, (2019) 115006.
- [35] S. Gardner, X. Yan, *Phys. Rev. D* **102**, (2020) 075016.
- [36] M. Badziak, K. Sakurai, *JHEP* **1910**, (2019) 024.
- [37] A. Hernandez, S. F. King, H. Lee, S. J. Rowley, *Phys. Rev. D* **101**, (2020) 115016.
- [38] A. Hernandez, Y. Velasquez, S. Kovalenko, H. N. Long, N. Perez-Julve, V. V. Vien, *Eur. Phys. Jour. C* **81**, (2021) 191.
- [39] S. Jana, S. Saad, *Phys. Rev. D* **101**, (2020) 115037.
- [40] L. Calibbi, M. Ibanez, A. Melis, O. Vives, *JHEP* **2006**, (2020) 087.
- [41] C. Chen, T. Nomura, *Nucl. Phys. B* **964**, (2021) 115314.
- [42] C. Chua, *Phys. Rev. D* **102**, (2020) 055022.
- [43] C. Hati, J. Kriewald, J. Orloff, A. M. Teixeira, *JHEP* **2007**, (2020) 235.
- [44] B. Dutta, S. Ghosh, T. Li, *Phys. Rev. D* **102**, (2020) 055017.
- [45] F. J. Botella, F. Cornet-Gomez, M. Nebot, *Phys. Rev. D* **102**, (2020) 035023.
- [46] I. Dorsner, S. Fajfer, S. Saad, *Phys. Rev. D* **102**, (2020) 075007.
- [47] S. Jana, W. Rodejohann, S. Saad, *Phys. Rev. D* **102**, (2020) 075003.
- [48] E. J. Chun, T. Mondal, *JHEP* **2011**, (2020) 077.
- [49] S. Li, X.-Q. Li, Y. Li, Y.-D. Yang, X. Zhang, *JHEP* **2101**, (2021) 034.
- [50] L. D. Rose, S. Khalil, S. Moretti, *Phys. Lett. B* **816**, (2021) 136216.
- [51] A. Hernandez, S. F. King, H. Lee, arXiv:2101.05819.
- [52] N. Chen, B. Wang, C. Yao, arXiv:2102.05619.
- [53] A. Bodas, R. Coy, S. King, arXiv:2102.07781.
- [54] J. Cao, Y. He, J. Lian, D. Zhang, P. Zhu, arXiv:2102.11355.
- [55] Y. Amhis et al. [Heavy Flavor Averaging Group (HFAG) Collaboration], arXiv:1412.7515.
- [56] S. Schael et al. [ALEPH and DELPHI and L3 and OPAL and SLD and LEP Electroweak Working Group and SLD Electroweak Group and SLD Heavy Flavour Group Collaborations], *Phys. Rept.* **427**, (2006) 257.

- [57] D. Eriksson, J. Rathsman, O. Stål, *Computl. Phys. Commun.* **181**, (2010) 189.
- [58] M. Tanabashi et al., [Particle Data Group], *Phys. Rev. D* **98**, 030001 (2018).
- [59] P. Bechtle, O. Brein, S. Heinemeyer, G. Weiglein, K. E. Williams, *Computl. Phys. Commun.* **181**, (2010) 138-167.
- [60] J. Alwall *et al.*, *JHEP* **1407**, (2014) 079.
- [61] P. Torrielli and S. Frixione, *JHEP* **1004**, (2010) 110.
- [62] J. de Favereau *et al.* [DELPHES 3 Collaboration], *JHEP* **1402**, (2014) 057.
- [63] D. Dercks, N. Desai, J. S. Kim, K. Rolbiecki, J. Tattersall and T. Weber, *Comput. Phys. Commun.* **221**, (2017) 383.
- [64] G. Pozzo and Y. Zhang, *Phys. Lett. B* **789**, (2019) 582-591.
- [65] A. M. Sirunyan *et al.* [CMS Collaboration], CMS-PAS-SUS-19-012.
- [66] DELPHI Collaboration (J. Abdallah et al.), *Eur. Phys. Jour. C* **38**, (2004) 1-28.